

EPR beams and photon number detector: Toward synthesizing optical nonlinearity

M. Sasaki,¹ K. Wakui,¹ J. Mizuno,¹ M. Fujiwara,¹ and M. Akiba¹

¹Quantum Information Technology Group, National Institute of Information and Communications Technology (NICT),
4-2-1 Nukui-kitamachi, Koganei, Tokyo 184-8795, Japan

We present the two kinds of experimental results. One is a continuous variable dense coding experiment, and the other is a photon number detector with high linearity response, the so called charge integration photon detector (CIPD). They can be combined together to be a potential tool for implementing the cubic phase gate which is an important gate element to synthesize the measurement induced nonlinearity for photonic quantum information processing.

PACS numbers:

I. INTRODUCTION

One of the important tasks in quantum optics and quantum information processing is to implement any desired optical nonlinearity. Currently available nonlinear media, however, suffer from weak strengths and high losses. It was recently shown that nonlinear interaction between photons can be implemented using linear optical elements, ancilla photons, and post selection based on the output of single-photon detectors, now referred to as the measurement induced nonlinearity. [1]. For example, a nondeterministic Kerr interaction can be effected in this way. Although this nondeterministic nonlinear interaction works only a fraction of total events, such operations can be performed off-line from the quantum computation.

This original idea has been extended recently for the continuous variables of photonic field [2, 3]. In [2], it was shown the cubic phase gate $\hat{V}_\gamma = \exp(i\gamma\hat{x}^3)$ where \hat{x} is the quadrature amplitude, can be implemented using the two mode squeezed state (EPR beams), the interactions specified by the Hamiltonians up to the bilinear order of the creation and annihilation operators $\{\hat{a}, \hat{a}^\dagger\}$, and the measurements by a photon number detector and a homodyne detector (see Fig. 1). It is also known that once a nonlinear Hamiltonian with a cubic or higher polynomial of $\{\hat{a}, \hat{a}^\dagger\}$ is obtained, it is possible to build up arbitrary multi-mode Hamiltonians by cascading this with the bilinear Hamiltonians and the beam splitters [4]. The bilinear Hamiltonians are more or less in a range of current technologies. A big challenge is to synthesize a nonlinear Hamiltonian such as the cubic phase gate. This gate opens the possibilities of implementing quantum operations not only on the photonic states in the discrete spectrum but also on the states in the continuous spectrum. The latter includes Gaussian input states which are essential signal carriers in optical communications.

We present our recent work on the two key elements for the cubic phase gate: the continuous variable dense coding experiment with the EPR beams and a photon number detector.

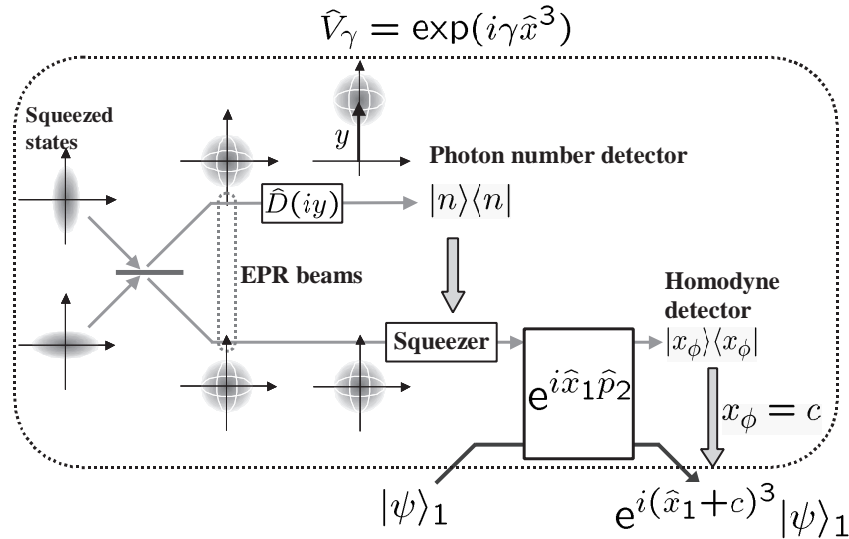


FIG. 1: Schematic diagram of the cubic phase gate based on the measurement induced nonlinearity.

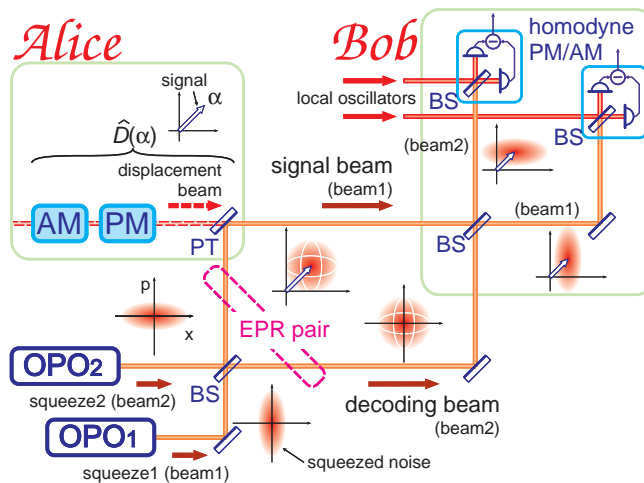


FIG. 2: Schematic diagram of dense coding experiment using squeezed vacuum states.

II. CONTINUOUS VARIABLE DENSE CODING

Figure I shows a circuit to implement the cubic phase gate. One of the EPR beams first undergoes the displacement operation described by the operator $\hat{D}(\alpha)$. One of the encoded EPR beams is then detected by a photon number detector with the precision satisfying $\Delta n \ll n^{1/3}$. The measurement result of n photons projects the other beam into a certain non-Gaussian state. This state is further transformed via a single mode squeezer, and is then coupled with a target input state $|\psi\rangle_1$ through a unitary process of a bilinear interaction $e^{i\hat{x}_1\hat{p}_2}$. One of the output mode is finally measured by a homodyne detection. According to the measurement result, the target state $|\psi\rangle_1$ can be modulated by the cubic phase shift.

It is still difficult to perform this whole operation. We first work on the preparation of the displaced EPR beams, and the characterization of them, which is nothing but the continuous variable dense coding scheme [5]. Its schematic is shown in Fig. II. Two independent squeezed vacua from the optical parametric oscillator (OPO) cavities are combined to create EPR beams. For the OPO, a 10 mm long potassium niobate (KNbO₃) crystal is employed. A light source is a Ti:sapphire laser (Coherent, MBR-110) whose fundamental wavelength is 860 nm. The OPO cavities are pumped by the second harmonic beam generated by a frequency doubler (Coherent, MBD-200). The two squeezed beams are generated at fundamental wavelength. One of the EPR beams is super-imposed via a high reflectivity mirror ($T_{PT} \approx 1\%$) with a bright beam with the amplitude and phase modulations. This setup realizes the displacement operation on the signal beam. The encoded EPR beams are decoded by the Bell measurement unit where the encoded EPR beams are first separated into two squeezed states via a 50:50 beamsplitter, and are then detected by two homodyne detectors to extract the signal in amplitude- and phase-quadratures.

The experimental results are shown in Fig. II. Figure II(a) shows the noise power of the two orthogonal quadratures around 1.1 MHz in the time domain. As seen, the EPR noise (ii) is larger than the shot noise (i) and also is phase independent. This EPR noise can be canceled in the Bell measurement, resulting into two separable squeezed states with about 2dB squeezing, (iii) and (iv), below the shot noise level. Figure II(b) shows the noise power spectra in the frequency domain. The AM and PM signals (iii) at 1.3 MHz and 1.1 MHz, respectively, buried in the vacuum noise (i) are decoded by the Bell measurement. Thus we have successfully performed encoding and decoding assisted by the entanglement in the two orthogonal quadratures.

III. CHARGE INTEGRATION PHOTON DETECTOR

Now we move to the other important element, a photon number detector. Many approaches have been taken to construct photon number resolving detectors. For the visible light region, there is a nice device called VLPC which has a very high quantum efficiency, and could directly observe nonclassical light statistics [6]. There are also several other candidates based on sophisticated mechanisms, such as quantum dot array FET [7], and the superconducting edge sensor [8]. Recently another practical scheme has been demonstrated, which is based on cascading commercially available Si-APDs [9, 10]. All these devices have both merits and demerits depending on our purposes.

Here we would like to add another candidate to this list. Our approach is very straightforward. We convert photons

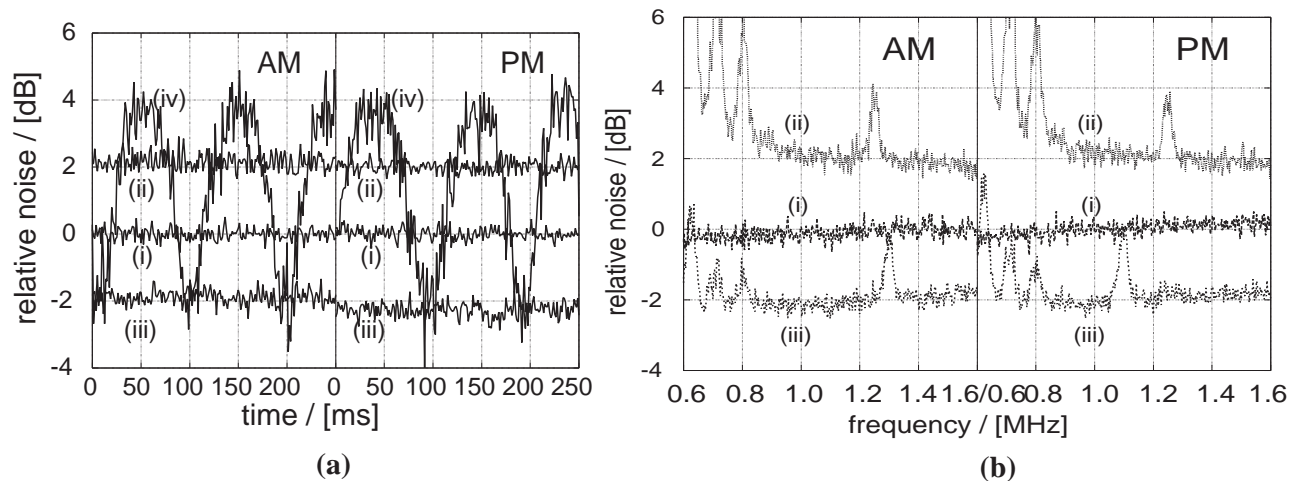


FIG. 3: (a) Outputs from the Bell measurement in the time domain; (i) shot noise, (ii) EPR noise, (iii) squeezed beam with LO locked, and (iv) squeezed beam. (b) Outputs from the Bell measurement in the frequency domain; (i) shot noise, (ii) EPR noise, and (iii) squeezed beam with LO locked. The vertical scale is normalized by the shot noise level around 1.1 MHz. The peaks at 1.25 MHz and in low frequency region (< 0.8 MHz) are due to the technical noises of the laser rather than the quantum noise.

into electrons with low noise using a photodetector at cryogenic temperature either Si-APD in the linear mode for the visible and near infrared window or InGaAs p-i-n photo-diode for the telecom-fiber window. We then amplify photo-electrons by a very low noise charge integration amplifier. We call this scheme the charge integration photon detector (CIPD).

In Fig. III(a), we show a schematic diagram of CIPD in the case of Si-APD for the visible and near infrared window. The readout circuit is based on a capacitive transimpedance amplifier, where we use a Si junction field effect transistor (JFET) as preamplifier, and a diode and a relay switch for reset. We removed as many of the materials and devices that generate leak current, stray capacitance, and dielectric polarization noises as possible from the circuit. As a result the readout circuit has ultralow current-noise at low frequencies and a low input capacitance of 1 pF. So the Si-APD can be operated at very low gains. We use it with the gain about 10, corresponding to the bias voltage of 90 V. The Si-APD used is a 200 μm -diameter bare chip made by Matsusada Precision Inc. The quantum efficiency is estimated to be about 60% at 635 nm wavelength, which was indirectly determined from the room-temperature quantum efficiency (69%) given in the manufacturer's catalog. That is, the drop of the output current at 77 K was compared with the one at room temperature.

Figure III(b) shows the photon number probability distributions for four kind of pulse intensities. (Precisely speaking, this corresponds to the number of input referred photoelectron. To convert them to the photon number probability distributions, we have to estimate the quantum efficiency more precisely.) These data were obtained by integrating the photoelectrons created by each pulse of 2,000 light pulse events with repetition of 20 Hz. The light source is a 635-nm light-emitting diode. Unfortunately, we could not have succeeded precise discrimination of photon number yet. At present we could have achieved very low noise characteristics, and high-linearity response to the number of incident photons. An upper-limit dark current of 1 e/s was obtained from the maximum variation of the output voltage in 1 sec at 77 K.

In order to distinguish photon number precisely, we have to reduce the readout circuit noise, currently 7 electrons at 20 Hz sampling rate, further by 1/3, so as to improve the S/N ratio greater than 4. This is possible by reducing the total stray capacitance of the system.

IV. CONCLUSION

We have presented two basic elements, the continuous variable dense coding experiment, and the charge integration photon detector (CIPD). They can be combined together to be a powerful tool for implementing the cubic phase gate which is an important gate element for photonic quantum information processing.

The authors acknowledge the financial support by the Ministry of Public Management, Home Affairs, Posts and

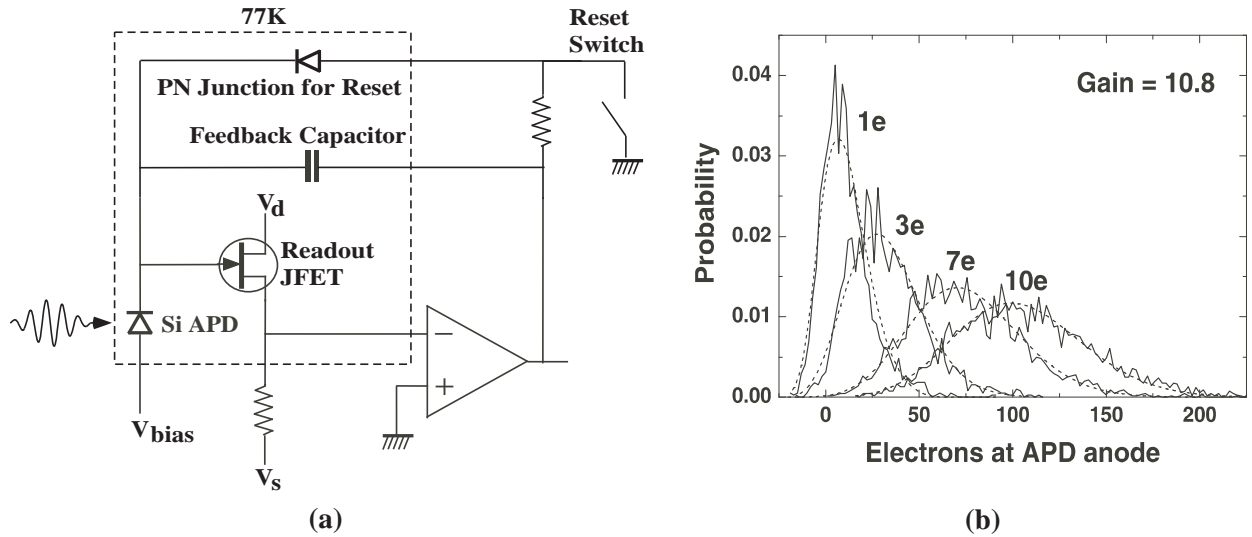


FIG. 4: (a) Schematic diagram of CIPD. (b) Probability distributions of photoelectron.

Telecommunications, and the CREST project of Japan Science and Technology.

-
- [1] K. Knill, R. Laflamme, and G. J. Milburn, *Nature* **409**, 46 (2001).
 - [2] D. Gottesman, A. Kitaev, and J. Preskill, *Phys. Rev. A* **64**, 012310 (2001).
 - [3] S. D. Bartlett and B. C. Sanders, *Phys. Rev. A* **65**, 042304 (2002).
 - [4] S. Lloyd and S. L. Braunstein, *Phys. Rev. Lett.* **82**, 1784 (1999).
 - [5] S. L. Braunstein and H. J. Kimble, *Phys. Rev. A* **61**, 042302 (2000).
 - [6] E. Waks, E. Diamanti, B. C. Sanders, S. D. Bartlett, and Y. Yamamoto *Phys. Rev. Lett.* **92**, 113602 (2004)
 - [7] A. J. Shields, M. P. O'Sullivan, I. Farrer, D. A. Ritchie, R. A. Hogg, M. L. Leadbeater, C. E. Norman, and M. Pepper, *Appl. Phys. Lett.* **76**, 3673 (2000).
 - [8] A. J. Miller, S. W. Nam, J. M. Martinis, and A. V. Sergienko, *Appl. Phys. Lett.* **83**, 791 (2003).
 - [9] D. Achilles, Ch. Silberhorn, C. Sliwa, K. Banaszek, and I. A. Walmsley, *Opt. Lett.* **28**, 2387 (2003).
 - [10] M. J. Fitch, B. C. Jacobs, T. B. Pittman, and J. D. Franson, *Phys. Rev. A* **68**, 043814 (2003).